

# Impact of cooling on the water mass exchange of Agulhas rings in a high resolution ocean model

J. Donners and S. S. Drijfhout

Royal Netherlands Meteorological Institute, De Bilt, Netherlands

A. C. Coward

Southampton Oceanography Centre, Southampton, UK

Received 1 June 2004; accepted 10 August 2004; published 31 August 2004.

[1] The leakage of water from three Agulhas rings has been studied in a high resolution global ocean model using a Lagrangian particle following technique. A bowl shaped ring boundary that reaches a radius of 140 km and a depth of 800 m separates regions of fast and slow leakage. The dilution of Agulhas ring water generally increases with depth, but a shallow secondary circulation enhances leakage in the upper 150 m. Strong surface cooling upsets the horizontal pressure gradient which is balanced by subinertial motions that act to form this shallow overturning cell. *INDEX TERMS*: 4255 Oceanography: General: Numerical modeling; 4504 Oceanography: Physical: Air/sea interactions (0312); 4520 Oceanography: Physical: Eddies and mesoscale processes. **Citation**: Donners, J., S. S. Drijfhout, and A. C. Coward (2004), Impact of cooling on the water mass exchange of Agulhas rings in a high resolution ocean model, *Geophys. Res. Lett.*, 31, L16312, doi:10.1029/2004GL020644.

## 1. Introduction

[2] The Agulhas Current is the strongest western boundary current of the southern hemisphere. It retroflects to the south of South Africa and flows back into the Indian Ocean as the Agulhas Return Current. Agulhas rings are shed off the retroflection loop irregularly and move into the South Atlantic Ocean in a north-westerly direction. These rings form an important link between the subtropical gyres of the South Atlantic Ocean and the Indian Ocean [*de Ruijter et al.*, 1999]. This link is thought to play an important role in the upper branch of the global thermohaline circulation [*Weijer et al.*, 1999]. *Schouten et al.* [2000] followed these rings with satellite measurements of sea surface height (SSH). During the first five months after the shedding of Agulhas rings the decay of the SSH is strongest. *Drijfhout et al.* [2003] showed that the strong decay is associated with a mixed barotropic/baroclinic instability. In most cases this instability leads to split-up of the ring. Loss of a passive tracer from the ring scales well with the decay of SSH.

[3] From theoretical considerations, *Flierl* [1981] concluded that, when the rotational speed is larger than the translational speed of the eddy, water is trapped inside eddies. This suggests that leakage across a ring boundary above a certain critical depth is weak, while it will be strong below this depth. Indeed, *van Aken et al.* [2003] discussing observations of a young Agulhas ring, found no systematic

differences of water mass properties between the ring and its surroundings below the 12°C isotherm, located at a depth of 650 m in this ring. The leakage of water from Agulhas rings below this depth has also been found in a numerical model of an Agulhas ring [*de Steur et al.*, 2004].

[4] Agulhas rings are strongly cooled, especially in winter. *Dewar* [1987] calculated the restructuring of an idealized warm ring using a two-layer model. Estimates of energy release during adjustment suggest that a significant amount of energy is converted into internal wave energy. *Drijfhout et al.* [2003], however, found that the effect of cooling is weak; the instability process develops marginally slower. An alternative theory was developed by *Young* [1994]. In his subinertial mixed layer (SML) theory, a balance arises between vertical mixing and “unmixing” by differential advection. The latter is associated with a sheared horizontal pressure gradient that may arise, for instance, from cooling.

[5] In this article we analyze the water mass exchange of three Agulhas rings in a high-resolution global ocean model. This enables us to look at the decay processes of Agulhas rings in a realistic setting. The model allows for a detailed vertical structure within the mixed layer, which has not been studied before. Water mass exchange between the ring and the surroundings is calculated with Lagrangian diagnostics.

## 2. Data and Methods

[6] The general circulation model OCCAM [*Webb et al.*, 1997] was used for a detailed study of Agulhas rings. The model uses an eddy-resolving resolution of 1/12° and employs 66 depth levels, with 20 layers in the top 200 m. The mixed layer is described by the KPP scheme [*Large et al.*, 1994]. The initial potential temperature and salinity fields were interpolated from the WOCE SAC climatology [*Gouretski and Jancke*, 1996] for most of the World’s oceans together with World Ocean Atlas data [*Antonov et al.*, 1998; *Boyer et al.*, 1998]. During the run analyzed here, the ocean surface was forced by a monthly average ECMWF wind stress climatology [*Gibson et al.*, 1997] calculated from the years 1986 to 1989 inclusive [*Siefridt and Barnier*, 1993]. Surface relaxation of temperature and salinity toward monthly climatologies [*Levitus et al.*, 1994; *Levitus and Boyer*, 1994] was also applied. The model was run for two years, of which the second year was used for our analysis. We used instantaneous model fields at three day intervals for all calculations.

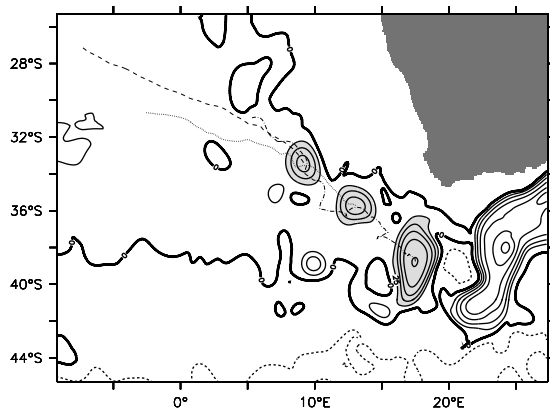


**Figure 1.** The initial position of the three Agulhas rings and their path in the following year. The contours at every 25 cm indicate the SSH, the light shaded area shows where the Lagrangian trajectories have been initialized. Dark shading indicates the African continent.

[7] For the Lagrangian analysis of leakage from Agulhas rings we used an off-line approach [Döös, 1995], extended by *de Vries and Döös* [2001] for the use with time-dependent flows. Every particle represents a specified volume of water ( $10^9 \text{ m}^3$ ). More than twenty thousand particles were used for the smallest Agulhas ring. Each trajectory was followed for the full second year of the model run. Particles were seeded in the top 2000 m of the Agulhas ring wherever the SSH was above 25 cm. The center of the Agulhas ring was defined as the interpolated location of the SSH maximum. The Agulhas rings were also analyzed in a two-dimensional, Eulerian framework. To this end, the data was azimuthally averaged around the ring center and plotted as a function of radial distance and depth.

### 3. Water Mass Exchange

[8] Figure 1 shows the SSH at the beginning of the year that has been used for the following analysis. The Agulhas Current is centered at  $24^\circ\text{E}$ . The light shading indicates the regions within the three Agulhas rings where Lagrangian particles were seeded. Also the path of the three rings has been indicated. The youngest (and largest) Agulhas ring is two weeks old. The ring properties (sea surface salinity, sea surface temperature, SSH, mixed layer depth or MLD, ring size and the depth anomaly of the  $12^\circ\text{C}$  isotherm) agree very well with Agulhas ring “Astrid” [van Aken *et al.*, 2003], so we conclude that the modeled rings are realistic. The ring breaks up after two months, and sheds some small rings in the following two months. The split-up can be attributed to the mechanism described by *Drijfhout et al.* [2003]. The middle ring was shed off mid-November, at the end of spring. The oldest ring was formed in mid-winter of the first year. The two oldest rings are stable and do not break up.

[9] The Agulhas rings have been traced with the Lagrangian particle technique for one year to investigate the leakage of water into the environment. Only the results of the middle ring (located at  $36^\circ\text{S}$ ,  $13^\circ\text{E}$ ) are shown here. All results are equally applicable to the other Agulhas rings, unless otherwise stated. Figure 2 shows the average

residence time (or  $e$ -folding time scale) of particles within the ring as a function of distance from the ring center and depth. For each azimuthally averaged gridcell an exponential function was fitted to the concentration of particles as a function of time. A clear, bowl shaped division can be seen between particles that reside in the ring (white) and particles that leak into the environment (dark gray). The bowl shape reaches to a distance of 140 km and a depth of 800 m. The decay of the anomalous heat and salt within the bowl is estimated with a linear extrapolation between 2 to 6 years.

[10] Figure 2 also shows the contour where the rotational velocity is at least twice the translational speed of the Agulhas ring. Note that the contour shallows at approximately 80 km distance from the ring center, where the maximum azimuthal velocity is largest. The criterion is a good indicator of the bowl shaped ring boundary. This criterion is also valid for the oldest ring, although for the largest ring it only holds for the period when no instabilities develop. The average residence time along the ring boundary is 250 days. The criterion of *Flierl* [1981] for the ring boundary, namely where the rotational speed equals the translational speed, is also shown on Figure 2 (lower contour). This reaches down to 1200 m and 20 km further outward. This criterion defines a less sharp boundary in terms of the average residence time, which can be attributed to the unsteadiness of both the ring boundary and its self advection [de Steur *et al.*, 2004].

[11] In the upper 150 m of the Agulhas ring a significantly stronger water mass exchange can be seen, in the form of a curl of water with a lower residence time. This suggests that the surrounding water is drawn into the ring at 100 m depth, upwells within the ring and flows radially outward near the surface. The streamfunction of the circulation causing the enhanced leakage near the surface is

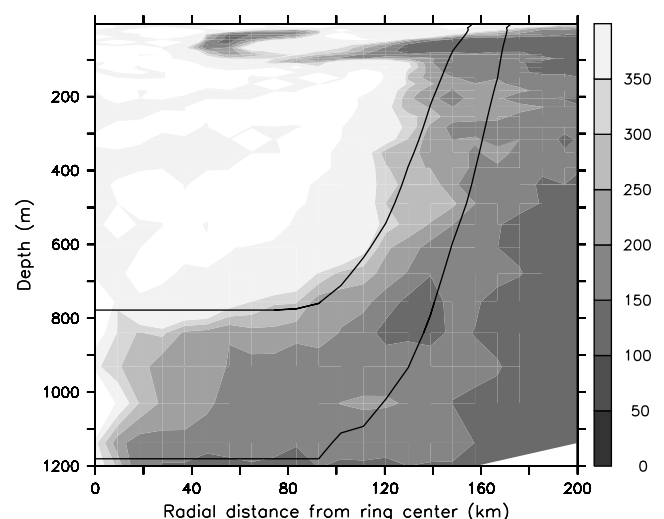


**Figure 2.** The figure denotes the average residence time (in days) of Lagrangian trajectories within an Agulhas ring. The upper contour indicates the location where the azimuthal velocity is at least twice the translational velocity of the ring. The lower contour indicates the location where the azimuthal velocity is equal or larger than the translational velocity of the ring. The contours define two different ring edges.

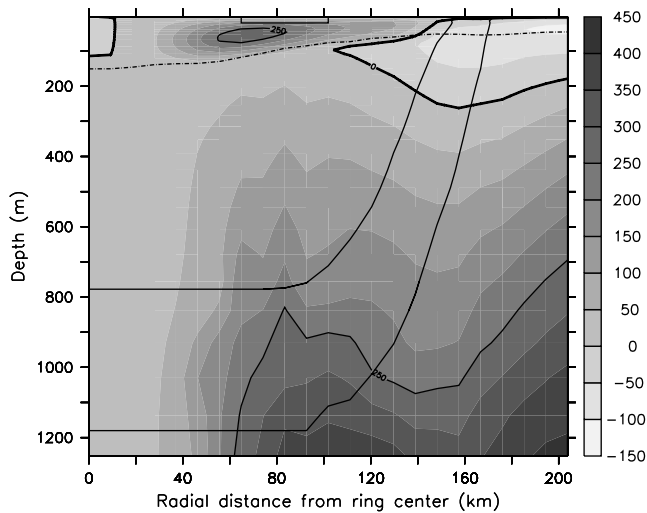


**Figure 3.** Streamfunction of the shallow overturning cell (in mSv) at the end of winter. Positive values indicate clockwise rotation. The MLD is indicated with the dash-dotted line.

shown in Figure 3. The shallow overturning cell is the strongest circulation feature within the bowl shaped ring boundary and is confined to the mixed layer. The cell is present in all Agulhas rings during winter and spring, when heat loss is strong. The overturning circulation in the mixed layer is independent of the azimuth angle (not shown).

#### 4. Mixed Layer Processes

[12] For a better understanding of the mechanism behind the secondary circulation described in the previous section, we calculated the different terms of the density balance:

$$\frac{\partial \rho}{\partial t} + u \frac{\partial \rho}{\partial r} + w \frac{\partial \rho}{\partial z} - \frac{\alpha Q}{c_w} - \beta S(P - E) - \Gamma = 0 \quad (1)$$

All variables were azimuthally averaged. The mixing term  $\Gamma$ , which includes all cross-correlational terms, was not calculated explicitly but equalled to the residual.

[13] The different terms of the density balance were calculated as a function of time in the top 11 m (upper two grid boxes), where the overturning cell and the atmospheric interaction are both strong. The density balance is plotted in Figure 4. There is a clear balance between the strong surface forcing and horizontal advection. The fresh-water forcing is weak and constant ( $5.7 \cdot 10^3 \text{ kg s}^{-1}$ ). Atmospheric cooling of the Agulhas ring in winter causes the strong surface forcing. The surface cooling of Agulhas rings increases in autumn and winter and diminishes during spring. The horizontal advection is directed radially outward at the surface. Dense (cold) water flowing radially outward is replaced by light (warm) water from the ring center. This balance also holds for the other two Agulhas rings. For the largest ring this balance is only established when no more instabilities develop.

[14] The surface cooling is strongest close to the ring center, but this heat loss is effectively distributed over the depth of the mixed layer by convection. Near the ring center the mixed layer is deeper, so the effective cooling of the

mixed layer is largest near the ring boundary where the mixed layer shallows. The maximum effective forcing coincides with maximum horizontal advection.

#### 5. Discussion

[15] The SML theory [Young, 1994] may explain how the overturning circulation arises. The buoyancy flux upsets the preexisting geostrophic equilibrium and the system moves towards a new geostrophically adjusted state. The resulting horizontal pressure gradient features strong vertical shear and subinertial motions balance this pressure gradient with vertically sheared advection. Shear-driven restratification operates most efficiently when the timescale of vertical mixing of momentum  $\tau_U$  is on the order of the inertial timescale  $f^{-1}$ , when the parameter  $\mu \equiv (f\tau_U)^{-1} \approx 1$ . The parameter  $\mu$  can be estimated from a relation between the Brunt-Väisälä frequency  $N^2$  and buoyancy  $B$  in combination with the Richardson number  $Ri$  [Young, 1994, equation 4.9]:

$$N^2 = \frac{\tau}{\tau_U} (1 + \mu^2)^{-1} f^{-2} \nabla B \cdot \nabla B \quad (2)$$

$$Ri \equiv \frac{N^2}{u_z^2 + v_z^2} = \frac{\tau}{\tau_U} \quad (3)$$

The variable  $\tau$  is the timescale of vertical mixing of temperature and salinity. During the cooling phase the parameter  $\mu$  is close to 1 for all rings, in agreement with the SML theory (Figure 5). At the onset and ending of the cooling phase  $\mu$  tends towards 0, indicating that momentum mixing weakens and the ageostrophic velocity decreases. For  $\mu \ll 1$ , the validity of equation (2) breaks down. The Richardson number  $Ri$  is lower than 0.25, which indicates that vertical mixing of temperature and salinity is more rapid than vertical mixing of momentum.

[16] The combined action of unbalanced motions and vertical mixing in the SML theory rapidly removes density

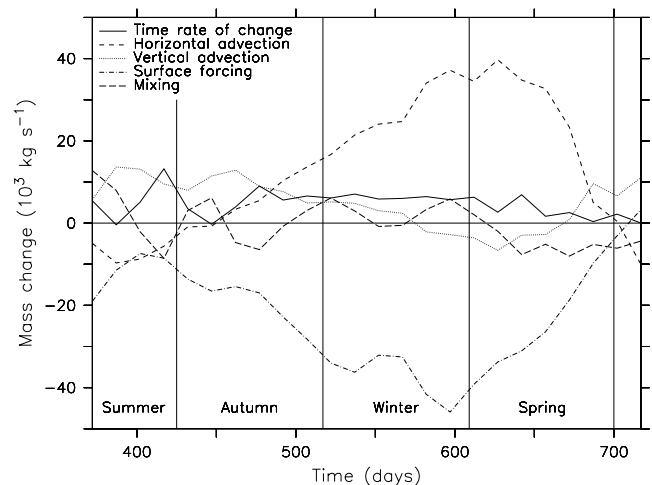


**Figure 4.** The mass budget as a function of time for the ring volume in the top 11 m of the Agulhas ring between 65 km and 102 km from the ring center (indicated in Figure 3).

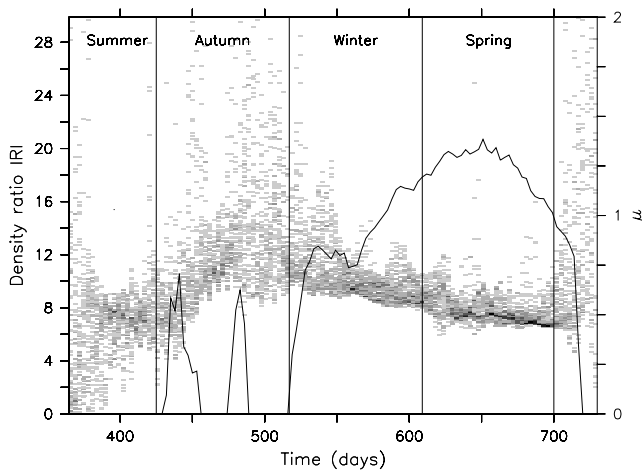


**Figure 5.** The distribution of the density ratio  $|R|$  in the shallow overturning cell of an Agulhas ring as a function of time. The thick line is the parameter  $\mu$ . The SML theory is applicable if  $\mu \approx 1$ .

gradients but leaves behind compensated temperature and salinity gradients. To test whether this process also applies here, we calculated the complex density ratio  $R$  according to Ferrari and Paparella [2003]:

$$R \equiv \frac{T_x + iT_y}{S_x + iS_y} \quad (4)$$

When gradients of temperature and salinity are compensated,  $|R|$  is equal to 1, while  $|R|$  is larger than 1 when temperature gradients determine the density gradients. Figure 5 shows the occurrence of  $|R|$  within the overturning cell. There is a preferred density ratio  $|R|$  of 8 and the alignment of temperature and salinity gradients is enhanced during the strong cooling phase (not shown). The Agulhas ring maintains the large scale radial temperature and salinity gradients, but the overturning circulation removes temperature and salinity gradients with other density ratios.

## 6. Conclusions

[17] We have analyzed the water exchange of three Agulhas rings during one year in an eddy-resolving global ocean model. There is a sharp boundary between particles that stay within the Agulhas ring and particles that mix into the environment. The ring boundary is well predicted by a criterion, based on Flierl [1981], that the azimuthal velocity is at least twice the translational velocity at any time. The original criterion of Flierl [1981] is less suited to indicate the ring boundary due to unsteadiness of the ring boundary and its self advection [de Steur et al., 2004]. The bowl shaped ring boundary reaches 140 km from the Agulhas ring center and down to 800 m. Below 800 m the Agulhas ring quickly loses its original water mass, in agreement with observations [van Aken et al., 2003]. The criterion for the ring boundary is not applicable to Agulhas rings that split due to a mixed barotropic-baroclinic instability [Drijfhout et al., 2003].

[18] Strong surface cooling generates a shallow overturning cell with radially outward flow near the surface

and a compensating inward flow at depth. The circulation is limited to the mixed layer. The cell can be explained by the SML theory of Young [1994]: cooling creates vertically sheared pressure gradients which induce vertically sheared subinertial motions. Vertical mixing is balanced by restratification due to the sheared flow. The overturning cell forms an effective pathway between the edge and the inside of the Agulhas ring and it amplifies the dilution of anomalous water properties of Agulhas rings near the surface. The surface water is not trapped in the core, but connected with the outside: the overturning cell amplifies this water mass exchange by constantly bringing new water to the edge where it is mixed with the environment.

[19] **Acknowledgments.** The research presented in this paper is supported by the Research Council for Earth and Life Sciences (ALW) of the Netherlands Organisation for Scientific Research (NWO), and is part of the MARE project and the CLIVARNET program. The model integrations are carried out as part of Southampton Oceanography Centre's core strategic research program which is supported by the UK's Natural Environment Research Council (NERC). The manuscript benefited strongly from the remarks of the reviewers.

## References

- Antonov, J. I., S. Levitus, T. P. Boyer, M. E. Conkright, T. D. O'Brien, and C. Stephens (1998), *World Ocean Atlas 1998*, vol. 1, *Temperature of the Atlantic Ocean*, NOAA ATLAS NESDIS 27, 166 pp., Natl. Oceanic and Atmos. Admin., Silver Spring, Md.
- Boyer, T. P., S. Levitus, J. I. Antonov, M. E. Conkright, T. D. O'Brien, and C. Stephens (1998), *World Ocean Atlas 1998*, vol. 4, *Salinity of the Atlantic Ocean*, NOAA ATLAS NESDIS 30, 166 pp., Natl. Oceanic and Atmos. Admin., Silver Spring, Md.
- de Ruijter, W. P. M., A. Biastoch, S. S. Drijfhout, J. R. E. Lutjeharms, R. P. Matano, T. Pichevin, P. J. van Leeuwen, and W. Weijer (1999), Indian-Atlantic interocean exchange: Dynamics, estimation and impact, *J. Geophys. Res.*, *104*, 20,885–20,910.
- de Steur, L., P. J. van Leeuwen, and S. S. Drijfhout (2004), Tracer leakage from modeled Agulhas rings, *J. Phys. Oceanogr.*, *34*, 1387–1399.
- de Vries, P., and K. Döös (2001), Calculating Lagrangian trajectories using time-dependent velocity fields, *J. Atmos. Oceanic Technol.*, *18*, 1092–1101.
- Dewar, W. K. (1987), Ventilating warm rings: Theory and energetics, *J. Phys. Oceanogr.*, *17*, 2219–2231.
- Döös, K. (1995), Interocean exchange of water masses, *J. Geophys. Res.*, *100*, 13,499–13,514.
- Drijfhout, S. S., C. A. Katsman, L. de Steur, P. C. F. van der Vaart, P. J. van Leeuwen, and C. Veth (2003), Modeling the initial, fast sea-surface height decay of Agulhas ring "Astrid," *Deep Sea Res., Part II*, *50*, 299–319.
- Ferrari, R., and F. Paparella (2003), Compensation and alignment of thermohaline gradients in the ocean mixed layer, *J. Phys. Oceanogr.*, *33*, 2214–2223.
- Flierl, G. R. (1981), Particle motions in large-amplitude wave fields, *Geophys. Astrophys. Fluid Dyn.*, *18*, 39–74.
- Gibson, R., P. Källberg, S. Uppala, A. Hernandez, A. Nomura, and E. Serrano (1997), 1997: The ERA description, the ECMWF re-analysis project report series, technical report, Eur. Cent. for Medium-Range Weather Forecasts, Reading, UK.
- Gouretski, V. V., and K. Jancke (1996), A new hydrographic data set for the South Pacific: Synthesis of WOCE and historical data, *Tech. Rep. 2*, WOCE Hydrog. Programme Spec. Anal. Cent., Hamburg, Germany.
- Large, W. G., J. C. McWilliams, and S. C. Doney (1994), Oceanic vertical mixing: A review and a model with a nonlocal boundary layer parameterization, *Rev. Geophys.*, *32*(4), 363–403.
- Levitus, S., and T. P. Boyer (1994), *World Ocean Atlas 1994*, vol. 4, *Temperature*, NOAA ATLAS NESDIS 4, 129 pp., Natl. Oceanic and Atmos. Admin., Silver Spring, Md.
- Levitus, S., R. Burgett, and T. P. Boyer (1994), *World Ocean Atlas 1994*, vol. 3, *Nutrients*, NOAA ATLAS NESDIS 3, 111 pp., Natl. Oceanic and Atmos. Admin., Silver Spring, Md.
- Schouten, M. W., W. P. M. de Ruijter, P. J. van Leeuwen, and J. R. E. Lutjeharms (2000), Translation, decay and splitting of Agulhas rings in the south-east Atlantic Ocean, *J. Geophys. Res.*, *105*, 21,913–21,925.
- Siefridt, L., and B. Barnier (1993), Banques de données AVISO vent/flux: Climatologie des analyses de surface du CEPMMT, *Tech. Rep. 91 1430 025*, Aviso, Ramonville St-Agne, France.

- van Aken, H. M., A. K. van Veldhoven, C. Veth, W. P. M. de Ruijter, P. J. van Leeuwen, S. S. Drijfhout, C. P. Whittle, and M. Roualt (2003), Observations of a young Agulhas ring, Astrid, during MARE in March 2000, *Deep Sea Res., Part II*, 50, 167–195.
- Webb, D. J., A. C. Coward, B. de Cuevas, and C. S. Gwilliam (1997), A multiprocessor ocean general circulation model using message passing, *J. Atmos. Oceanic Technol.*, 14, 175–183.
- Weijer, W., W. P. M. de Ruijter, H. A. Dijkstra, and P. J. van Leeuwen (1999), Impact of interbasin exchange on the Atlantic overturning circulation, *J. Phys. Oceanogr.*, 29, 2266–2284.
- Young, W. R. (1994), The subinertial mixed layer approximation, *J. Phys. Oceanogr.*, 24, 1812–1826.
- 
- A. C. Coward, James Rennell Division for Ocean Circulation and Climate, Southampton Oceanography Centre, European Way, Southampton SO14 3ZH, UK. (acc@soc.soton.ac.uk)
- J. Donners and S. S. Drijfhout, Department of Oceanographic Research, Royal Netherlands Meteorological Institute, Wilhelminalaan 10, De Bilt, 3732 GK, De Bilt, Netherlands. (donners@knmi.nl; drijfhou@knmi.nl)